Available online at www.sciencedirect.com
ScienceDirect
Ceramics International 35 (2009) 3455–3461
CERAMICS INTERNATIONAL
www.elsevier.com/locate/ceramint

Sintering of aluminum nitride by using alumina crucible and $MoSi_2$ heating element at temperatures of 1650 °C and 1700 °C

Chih-Hung Chu [a], Chih-Peng Lin [b,*], Shaw-Bing Wen [c], Yun-Hwei Shen [a]

[a] Department of Resources Engineering, National Cheng Kung University, No. 1 University Road, Tainan City 70101, Taiwan
[b] Department of Environment and Resources Engineering, Diwan College of Management, No. 87-1, Nanshih Li, Madou Town, Tainan County 72153, Taiwan
[c] General Education Center, Meiho Institute of Technology, No. 23, Pingguang Road, Neipu, Pingtung 91202, Taiwan

Received 2 April 2009; received in revised form 11 April 2009; accepted 24 June 2009
Available online 16 July 2009

Abstract

Aluminum nitride (AlN) ceramics, prepared with Y_2O_3 and CaO sintering additives, have been densified in an Al_2O_3 crucible at temperatures of up to 1650 °C and 1700 °C using a conventional $MoSi_2$ heating element furnace. The results of this study show that relative densities in excess of 99% of theoretical and a relatively high-thermal conductivity of 147 W m^{-1} K^{-1} have been achieved for feedstock materials prepared with combined addition of 1 wt.% Y_2O_3 and 1 wt.% CaO. All of the phases in sintered samples have been shown to be crystalline AlN and minor amount of secondary phases, were detected such as enriched Y- and Ca-aluminates by the XRD patterns, back-scattered imagery and microprobe analysis. The advantage of using the particular experimental system and sintering condition is considered to be amenable to lower production cost and enhance the feasibility of mass production. Critical temperature for AlN densification to obtain the highest density is about 1650 °C.

Keywords: C. Thermal conductivity; D. Al_2O_3; D. Y_2O_3; AlN

1. Introduction

Aluminum nitride (AlN) has attracted much attention, mainly because of its high-thermal conductivity. Slack [1] had calculated that AlN should have a theoretical room temperature thermal conductivity of 319 W m^{-1} K^{-1}, which is 90% and 7 times for that of BeO and Al_2O_3, respectively. Generally speaking, the thermal conductivity of AlN has been shown to give a wide range of values, the highest being 285 W m^{-1} K^{-1} for very pure single crystal [2]. This is especially true for polycrystalline AlN, where values range from less than 10–260 W m^{-1} K^{-1} depending on processing and purity [3]. However, AlN is difficult to sinter due to its high covalent bonding. For full densification, rare-earth and/or alkaline earth oxides are often added as sintering additives in the fabrication of AlN ceramics [4,5]. Watari et al. [6,7] demonstrated that additives of CaO and $LiYO_2$, priorly synthesized by mixing Y_2O_3 and Li_2CO_3 powders, has been shown to promote AlN densification at a low-temperature of 1600 °C. The authors have reported that the atomic weight of the rare-earths, as yttrium, samarium, and gadolinium element may substantially affect the apparent density of the sintered AlN specimen due to the kinetics of atomic diffusion during sintering, particularly for the mixture of Y_2O_3 and CaO addition [8].

Sintering of AlN has usually been carried out by different conventional equipments such as graphite furnace, tungsten furnace, spark plasma and microwave sintering furnace using different kinds of crucibles (graphite, AlN or BN) with or without a protective powder bed around the samples [9–17]. The batch-type processing system for obtaining high density AlN ceramics is generally considered to require high production cost. On the other hand, if dense AlN ceramics are to be fired in a box-type furnace, $MoSi_2$ can be used as heating element, rendering advantages of smaller size and simpler structure of the sintering furnace and, furthermore, a continuous firing may be applicable for mass production. U-shaped $MoSi_2$ heating elements may be chosen for their high maximum operating temperature of over 1800 °C in a weakly oxidizing environment. The electrical resistance of $MoSi_2$ heating element depends strongly on the element temperature [18]. The resistance curve increases sharply with temperature,

* Corresponding author. Tel.: +886 6 2095706; fax: +886 6 2380421.
E-mail addresses: erwinlin@mail.dwu.edu.tw, n4895108@mail.ncku.edu.tw (C.-P. Lin).

0272-8842/$36.00
doi:10.1016/j.ceramint.2009.06.026

being very useful for estimating temperature of the heating element as calculated from electrical resistance.

The objectives of this study are to improvise the conventional procedure so that the densification of AlN may be achieved by the deployment of a protective powder coating consisting of carbon black (C) and boron nitride (BN) in an alumina crucible; additives of Y_2O_3 and CaO have been used to promote the pressureless liquid-phase sintering. It should be pointed out the processing system of this experimentation has been aimed at the adoption of energy-saving operations including a relatively lower temperature range of 1600 °C, 1650 °C, and 1700 °C and using a box-type furnace equipped with a $MoSi_2$ heating element in nitrogen atmosphere.

2. Background for development of sintering condition

In previous works [10–14,17], Y_2O_3, CaO, and Li_2O have been employed as sintering additives for sintering of AlN ceramics, obtaining dense specimens with a thermal conductivity of up to 150 W m^{-1} K^{-1} by pressureless sintering using different kinds of crucibles (graphite, AlN or BN) equipped with graphite, tungsten, and microwave furnace with a flowing high-purity nitrogen atmosphere. However, the above systems under ambient atmosphere at high temperatures will result such undesirable effects of oxidation and decomposition of AlN pellets inside crucibles. On the consideration of lowering expenses in experimentation, this study has shown that it is feasible to employ an alumina (Al_2O_3) crucible with protective powder beds, namely carbon black and boron nitride powders, sintered in a box-type furnace with a conventional flow of nitrogen gas.

It is most important to evaluate the thermodynamics of oxidation effects for the sintering of AlN in the presence of different chemical materials such as C, B, Al, Ca, and Y. As such, the Ellingham diagram of Fig. 1, is useful in showing the change of standard free energy of oxidation reaction ΔG° vs. temperature, as provided by published data [19,20].

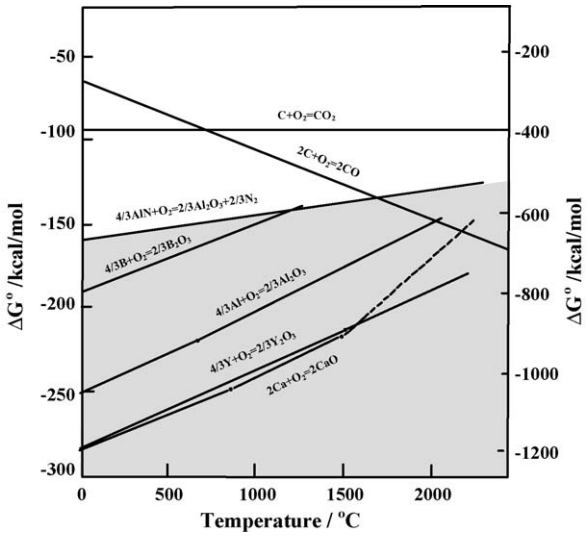

Fig. 1. Ellingham diagram of the related oxidations of AlN ceramics and metals (CaO and Y_2O_3 exist in the shaded zone and do not induce oxidation of AlN ceramics during firing) [18,19].

As shown in Fig. 1, the ΔG° of different chemical entities will invariably change with increase of temperature. However, the presence of amorphous carbon, as protective covering on the top of AlN feedstock in an Al_2O_3 crucible, serves the most indispensable function in preventing the oxidation of AlN by O_2 gas in the ambient atmosphere, as shown in the following reaction:

$$C_{(s)} + O_{2(g)} = CO_{2(g)} \quad (1)$$

$$2C_{(s)} + O_{2(g)} = 2CO_{(g)} \quad (2)$$

It may be noted in Fig. 1 that ΔG° seems to significantly decrease with the rise of temperature, this promoting the rate of CO gas formation; and the presence of CO gas is considered to be helpful in augmenting the reducing capability in the system.

In relation to the innovative use of Al_2O_3 crucible in our experimentation, the reactions given in Fig. 1 and Eqs. (3) and (4) seem to indicate that the ΔG° are increasing with the rise of temperature, implying that Al_2O_3 is relatively inert in the thermal system. The related equations are as follows:

$$(4/3)AlN_{(s)} + O_{2(g)} = (2/3)Al_2O_{3(s)} + (2/3)N_{2(g)} \quad (3)$$

$$(4/3)Al_{(s)} + O_{2(g)} = (2/3)Al_2O_{3(s)} \quad (4)$$

It is important to note that even though this study is somewhat unique in promoting lower overall processing costs; however, various significant aspects need to be given, such as field of thermodynamic consideration, low-temperature sintering by low-melting aid and very fine particle. Due to the necessity of extra extended presentation, it seems these aspects should be treated in further follow-up works.

3. Experimental procedure

The starting material was an AlN powder with specific surface area of 1.6 m^2/g, particle size (D_{50}) of 0.83 μm, and an oxygen impurity content of 2.2 wt.%, was used as feedstock. The AlN powder was mixed with 1 wt.% Y_2O_3 powder (Alfa Aesar, 99.9%, D_{50}: 7.23 μm), and 1.8 wt.% $CaCO_3$ (J.T. Baker, 99.8%, D_{50}: 16.38 μm, corresponding to 1 wt.% CaO) using as sintering additives. The powder mixture and PVB binder were mixed by vibration milling for 6 h using ethanol as a mixing medium. After drying and passing through a 100-mesh sieve. The powder mixture after granulation was uniaxially die pressed at 40 MPa into a pellet of 16.5 mm in diameter and 2 mm in thickness, and they were cold isostatically pressed (CIPed) under 98 MPa and dewaxed at 550 °C.

Fig. 2 shows the schematic representation of the arrangement of test specimens together with the Al_2O_3 crucible. The pellet was embedded in boron nitride (AVOCADO, 99%) powder bed which was sandwiched by BN plates, was placed in an Al_2O_3 crucible (SSA-S, 280 cm^3) being completely enveloped by a carbon black (Alfa Aesar, 99.9%) powder bed. The samples were sintered at 1600 °C, 1650 °C, and 1700 °C for 3 h, in a $MoSi_2$ heating furnace with a conventional flow of nitrogen atmosphere (Yunshan Co. Ltd., purity 95%).

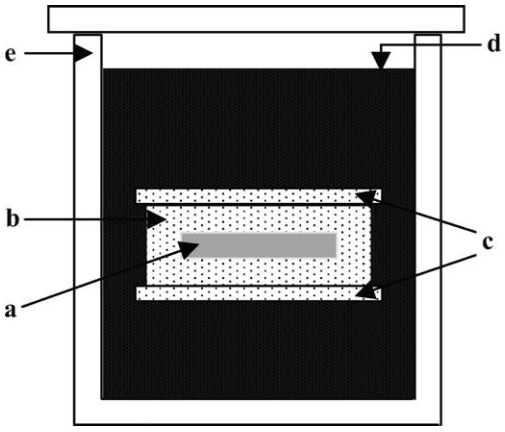

Fig. 2. Schematic representation of the arrangement of test specimen (a) together with the protective materials of BN (b and c) and carbon black (d) placed in an Al_2O_3 crucible (e).

The apparent densities of the sintered AlN were measured by using the Archimedes method. X-ray diffraction analysis (XRD, Siemens D5000) was employed to identify the evolved phases in each specimen. The lattice parameters of each sample was obtained by scanning from 20° to 80°, a step size of 0.02° 2θ/s and a sampling time of 8 s/step using XRD with Cu Kα radiation and the oxygen content of each specimen was measured by using N/O analyzer (LECO, TC-300). Microstructural characterization was observed by a scanning electron microscope (SEM) and back-scattered electron imagery (BSI, Hitachi S-3000N). Thermal diffusivities were measured using a laser flash thermal constant analyzer (Laser Flash LFA-447) and the thermal conductivity at room temperature was calculated from the equation $K = C\upsilon d$, where C is specific heat, υ is thermal diffusivity, and d is density of the sample (ASTM E1461).

4. Results and discussions

4.1. Phase compositions

Fig. 3 shows the X-ray diffraction spectra obtained after heat treatment of the green bodies at the temperature 1650 °C and 1700 °C for 3 h. The sample with 1 wt.% Y_2O_3 and 1 wt.% CaO addition, sintered at 1650 °C consists of AlN as predominant phase and trace amount of $CaAl_4O_7$ and $Y_3A1_5O_{12}$ as secondary phases, transforming to $CaAl_{12}O_{19}$ at 1700 °C. Among the XRD intensities of secondary phases, the phase $CaAl_{12}O_{19}$ (3) of seems to be much prominent than that of $CaAl_4O_7$ (1) and $Y_3A1_5O_{12}$ (2).

4.2. Densification of sintered AlN

The green densities of the powder compacts were approximate 54% TD for the all samples. It is shown in Fig. 4 that the densities of the specimens increase steadily with increase of the sintering temperature from room temperature to 1650 °C. It is noted that there seems to be a critical temperature for obtaining the highest density (above 99% of theoretical

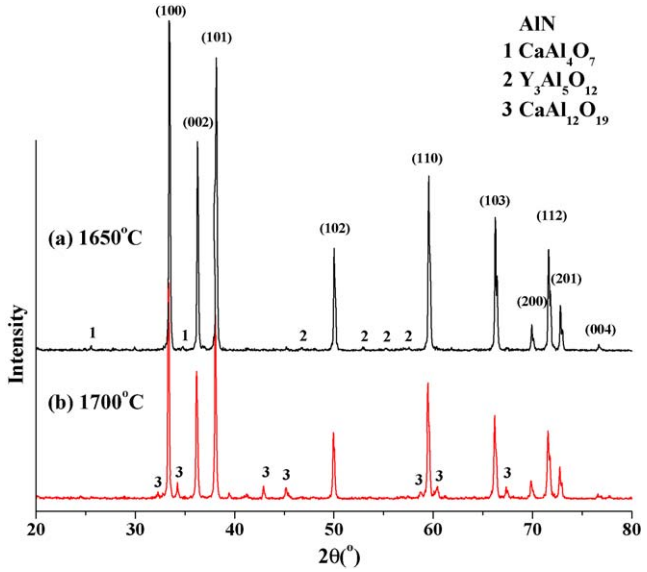

Fig. 3. X-ray diffraction profiles of sample with 1 wt.% Y_2O_3 and 1 wt.% CaO addition, was sintered at (a) 1650 °C and (b) 1700 °C for 3 h. AlN phase is shown by the indices as given in (a).

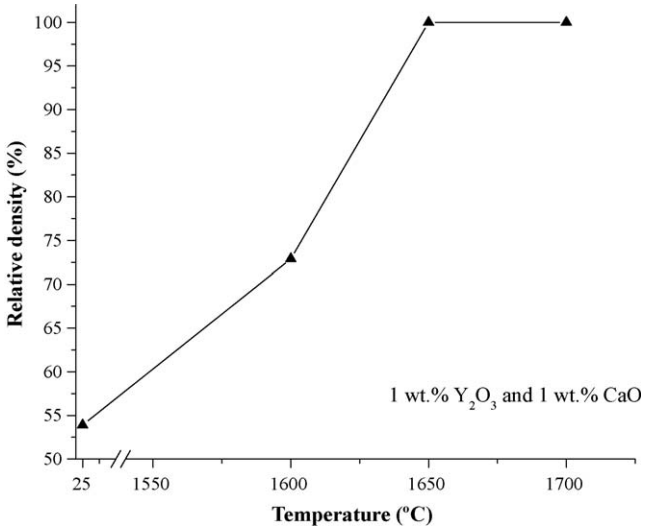

Fig. 4. The relative density of the sample with 1 wt.% Y_2O_3 and 1 wt.% CaO addition fired at various sintering temperature for 3 h.

values) seems to be around 1650 °C for the series of test runs. Whereas, the higher sintering temperature of 1700 °C has not been shown to be helpful to the further densification of AlN specimens. The demonstration of the critical temperature is clearly given in Fig. 4.

It should be pointed out that, comparatively speaking, the results for this and various studies [9–17] as tabulated in Table 3 show that 1650 °C, may be designated as the critical temperature, this being the lowest sintering temperature for obtaining the highest densification. The above results confirm that the fast densification rate for AlN–Y_2O_3–CaO system may be promoted by the formation of phases of $Y_3A1_5O_{12}$, $CaAl_4O_7$ and $CaAl_{12}O_{19}$ (by XRD patterns) that have melting point at lower than the critical temperature of 1650 °C. The use of other additives, such as Li_2O [7,14] or Sm_2O_3 [16] may also render

Table 1
Oxygen content, lattice constant c, and thermal conductivities of samples sintered at 1650 °C and 1700 °C for 3 h.

Temperature (°C)	Oxygen content[a] (wt.%)	O/N ratio[a]	Lattice constant (c) (Å)	Thermal conductivity (W m^{-1} K^{-1})
1600	n.a.	n.a.	n.a.	n.a.
1650	3.2	0.090	4.9755 (0.0003)	83.1
1700	3.6	0.079	4.9753 (0.0008)	146.5

[a] Determined by the N/O analyzer, n.a. = not available.

the lowest sintering temperature of 1600 °C, 1650 °C and 1500 °C, respectively. In addition, it has been indicated that precursor fine particle included raw AlN powder [21]; the function of additives as Y_2O_3 [22] or AlN [23] are also noted to be beneficial for lowering temperature.

4.3. Effect of oxygen concentration on thermal conductivity

A reduction of the lattice parameter (c) corresponds to higher oxygen concentration and lower thermal conductivity of the AlN grains [1,24]. An increase in the O/N ratio means an increase in the bulk defect caused by aluminum vacancies related to the increase in oxygen impurity.

Table 1 gives the thermal conductivities for the sample separately treated at two temperature levels, as 1650 °C and 1700 °C for 3 h. The results shown that specimen with 1 wt.% Y_2O_3 and 1 wt.% CaO addition at 1700 °C has the highest thermal conductivity at 146.5 W m^{-1} K^{-1}; for sample at 1650 °C given lower values of 83.1 W m^{-1} K^{-1}.

It may be recognized that the different values of thermal conductivities for the same ratio of additives of Y_2O_3 and CaO; and this generates different microstructures giving secondary as well as minor phases. Details for this phenomenon are given in the following sections of microstructures by SEM/BSI and chemistry by microprobe analyses. In our previous study [8], it has been shown the three rare-earths, as yttrium, samarium, and gadolinium element are useful additives for diffusion in sintering. Thus, it is considered that future experimentation may be helpful for evaluating the benefits of sintering by using other rare-earth elements.

4.4. Microstructures by SEM and back-scattered imagery

As shown in Fig. 5(a) and (b), respectively, the SEM photographs of fracture surfaces of specimen having the addition of Y_2O_3 at 1 wt.% and CaO at 1 wt.%, sintered at 1650 °C and 1700 °C for 3 h show no residual porosity and being fully consistent with the measurement values for the densities of sintered AlN.

Back-scattered SEM photographs of polished surface from the samples fired at 1650 °C and 1700 °C are shown in Fig. 5(c) and (d), the brighter color spots corresponds to the heavier Y- and Ca-rich secondary phases and the dark gray one corresponds to the relatively lighter aluminum nitride matrix. Virkar et al. [10] reported that the thermal conductivity of a multiphase material depends not only on the thermal

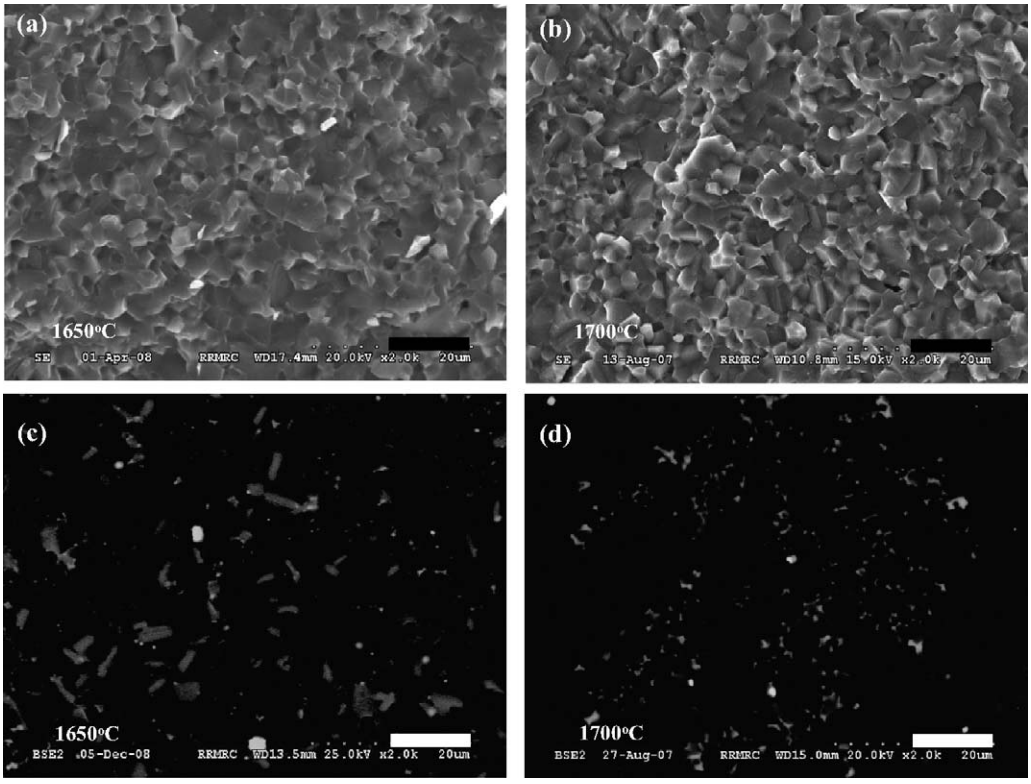

Fig. 5. SEM fractographs (a) and (b) and back-scatter SEM micrographs (c) and (d) of the sample with 1 wt.% Y_2O_3 and 1 wt.% CaO sintered at: (a) and (c) 1650 °C; and (b) and (d) 1700 °C. The bright spots in (c) and (d) represent the minor phases, having Y_2O_3 and CaO additives (bars = 10 μm).

conductivities of the individual phases but also on their distribution.

It can be shown in Fig. 5(d) that the form of secondary phases isolated AlN grains are spot, indicating the high-thermal conductivity AlN grains obviously contact with each other; whereas, Fig. 5(c) shown to the highly conductive AlN grains are surrounded by the low thermal conductivity secondary phases, thus giving a lower effective thermal conductivity at 83.1 W m^{-1} K^{-1}. This particular specimen gives a highest value of thermal conductivity at 147 W m^{-1} K^{-1}; seemly, the presence of more secondary phase from sintering 1650 °C is thus shown to be a hindrance to thermal conductivity.

4.5. Microprobe analyses for minor phases

Fig. 6 shows the chemical element distribution of the morphology of secondary phases performed by line scanning attached to a SEM. It is observed that the lightly color region (location a) is identified Ca, Al, and O element, as the elements making up the grain boundary phase, and the bright color region (location b) is consisted of Y–Al compound in having Y_2O_3 are showing brighter spots. Furthermore, it is believed that the additive Y_2O_3 can promote grain boundary diffusion [8], giving the optimum distribution of grain boundary phases located at AlN grains, achieving relative higher AlN thermal conductivity.

4.6. The advantages of Al_2O_3 crucible and $MoSi_2$ heating element

Cost comparison for different heating elements for sintering of aluminum nitride is shown in Table 2; a SiC heating element is known to be the cheapest. However, in this research, the advantage of using a $MoSi_2$ heating element implies that the furnace can be designed in having simple construction as well as smaller volume, so that lower production cost together with advantage of continuous firing for mass production may be possible.

Table 3 summarizes the relationship between the thermal conductivity and the oxygen content of AlN specimens obtained under different sintering conditions. It can be noted that the oxygen contents in the starting powder (i.e., below 1.5 wt.%) of previous reports are much lower than that of this study (i.e., 2.2 wt.%). Furthermore, an excessively high temperature up to 1800 °C was needed for the same study [9–11,13,15,17].

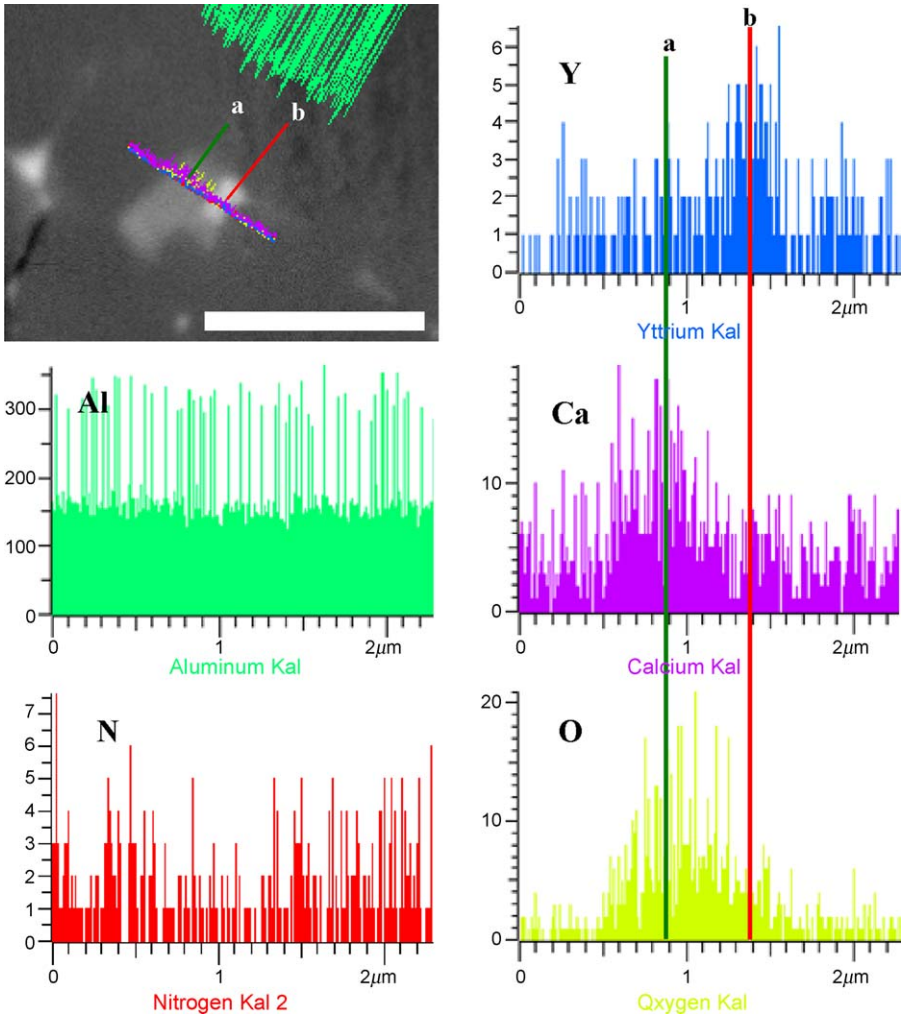

Fig. 6. Chemical element characterization of the morphology of secondary phases in the sintered AlN observed by line scanning of SEM. Points of (a) and (b) represent the actual position in the specimen (bars = 3 μm).

Table 2
Comparison with heating element for sintering of aluminum nitride.

System			Operation			References
Heating element	Material cost	Construction of equipment	Sintering temperature (°C)	Ramping rate	Atmosphere	
$MoSi_2$	*Low*	*Simple*	1700	*Slow*	*Ambient*	*This study*
SiC	Lowest	Simple	1500	Slow	Ambient	None
Tungsten	High	Complicated	1900	Medium	N_2	[11]
Graphite	High	Complicated	1650–1880	Medium	Vacuum, N_2	[10,12–15]
Spark plasma	High	Complicated	1500	Quick	Vacuum	[16]
Microwave	High	Complicated	1800	Quick	N_2	[17]

Table 3
Phases and properties of sintered AlN.

Sintering condition			Additives	Phases	Total oxygen content (wt.%)	Properties	References
Kinds of crucibles	Powder bed	Setting and sintering temperature				Thermal conductivity ($W\ m^{-1}\ K^{-1}$)	
Al_2O_3	*BN, carbon black*	1700 °C *for* 3 h, *$MoSi_2$ heating furnace in N_2 gas.*	*Y_2O_3–CaO*	*AlN, $CaAl_{12}O_{19}$, trace of $Y_3Al_5O_{12}$ (YAG)*	3.6	147	This study
Graphite	BN	1800 °C for 2 h, hot-pressed under 100 kg/cm^2 pressure in 1 atm of N_2 gas.	CaC_2	AlN	0.22	180	[9]
AlN		1850 °C for 100 min, graphite heating element in N_2 gas.	Y_2O_3	AlN, $Y_4A_{l2}O_9$ (YAM), trace of Y_2O_3	1.1	194	[10]
Carbon foils		1900 °C for 5 h, tungsten resistance furnace in a 0.1 MPa N_2 gas.	Y_2O_3	n.g.	0.1	220	[11]
BN-coated graphite		1770 °C for 2 h, graphite heating in N_2 gas at 1 MPa.	Y_2O_3	n.g.	n.g.	194	[12]
Graphite	AlN	1880 °C for 2 h, graphite heating element in N_2 gas.	Y_2O_3	AlN, $Y_3Al_5O_{12}$ (YAG), $Y_4Al_2O_9$ (YAM), $YAlO_3$ (YAP), Y_2O_3	1.63	154	[13]
BN		1650 °C for 8 h, graphite heating element in N_2 gas.	CaF_2–Y_2O_3–Li_2O	$CaYAlO_4$, $CaYAl_3O_7$	n.g.	167	[14]
Graphite		1830 °C for 6 h, graphite heating element in N_2 gas.	Sm_2O_3	n.g.	n.g.	166	[15]
		1500 °C for 3 min, spark plasma sintering in vacuum	Sm_2O_3	$SmAlO_3$	n.g.	118	[16]
AlN	AlN	1800 °C for 30 min, microwave sintering in N_2 gas.	Y_2O_3	AlN, $YAlO_3$ (YAP), $Y_4Al_2O_9$ (YAM)	1.3	169	[17]

Seemingly, this sintering system has been able to obtain an AlN product using lower temperature as well as cheaper, overall costs by the use of Al_2O_3 crucible and $MoSi_2$ heating element. The above product has a slightly lower thermal conductivity at 147 $W\ m^{-1}\ K^{-1}$ as opposite to that of other studies, giving range of thermal conductivities of 160–200 $W\ m^{-1}\ K^{-1}$. It should be pointed out that a product with a slightly lower thermal conductivity may be adequately enough for a range of applications.

5. Conclusions

1. The present work has demonstrated that AlN ceramics can be successfully densified using an alumina (Al_2O_3) crucible and a conventional $MoSi_2$ heating element furnace, thus avoiding the requirement of extra expenses by using controlled atmosphere in furnaces. It is noted that this method may be suitable for lowering the cost of preparation of AlN ceramics, using either a batch or continuous belt furnace, without the need for a controlled high-purity N_2 atmosphere.
2. With appropriate additives, namely 1 wt.% Y_2O_3 and 1 wt.% CaO, the AlN ceramic body gives very high density, approaching theoretical density of AlN (higher than 99%) and the same has a thermal conductivity of 147 $W\ m^{-1}\ K^{-1}$. Seemingly, the beneficial function of Y_2O_3 and CaO has been related to the formation of secondary minor phases of $CaAl_4O_7$, $Y_3Al_5O_{12}$, and $CaAl_{12}O_{19}$ that are related to lowering sintering temperature as well as capturing of oxygen in the system.
3. Considering the temperature for AlN densification for obtaining a product with a density of 99% (theoretical), the critical temperature is around 1650 °C.

Acknowledgments

This work is supported in part by the National Science Council (NSC 94-2622-E-434-002-CC3). The authors sincerely thank Prof. C.S. Huang for CIPed operation, Prof. S.L. Chung for N/O analysis, Prof. C.Y. Huang for lattice parameters *c* calculation in their laboratories, and Yonyu Applied Technology Material Co., Ltd. for the measurements of thermal conductivity. We sincerely wish to thank Dr. H.S. Liu for discussion and improving the English writing.

References

[1] G.A. Slack, Nonmetallic crystals with high thermal conductivity, J. Phys. Chem. Solids 34 (1973) 321–335.
[2] G.A. Slack, R.A. Tanzilli, R.O. Pohl, J.W. Vandersande, The intrinsic thermal conductivity of AlN, J. Phys. Chem. Solids 48 (7) (1987) 641–647.
[3] A. Horiguchi, F. Veno, M. Kasori, K. Shinozaki, A. Tsuge, Effect of sintering atmosphere on thermal conductivity and its microstructure for an AlN Ceramics, in: Proceedings of the 25th Symposium on the Basic Science of Ceramics, ID03, Yog Kyokai, (1987), p. 155.
[4] K. Komeya, H. Inoue, A. Tsuge, Role of Y_2O_3 and SiO_2 additions in sintering of AlN, J. Am. Ceram. Soc. 54 (1974) 411–412.
[5] K. Komeya, A. Tsuge, A. Inoue, Effect of $CaCO_3$ addition on the sintering of AlN, J. Mater. Sci. Lett. 1 (1986) 325–326.
[6] K. Watari, H.J. Hwang, M. Toriyama, S. Kanzaki, Low-temperature sintering and high thermal conductivity of $YLiO_2$-doped AlN ceramics, J. Am. Ceram. Soc. 79 (1996) 1979–1981.
[7] K. Watari, H.J. Hwang, M. Toriyama, S. Kanzaki, Effective sintering aids for low-temperature sintering of AlN ceramics, J. Mater. Res. 14 (1999) 1409–1417.
[8] C.H. Chu, Y.H. Shen, C.P. Lin, S.B. Wen, Effects of additives of CaO and rare-earth oxides on the sintering behavior of AlN ceramics, J. Kor. Phys. Soc. 52 (2008) 1545–1549.
[9] Y. Kurokawa, K. Utsumi, H. Takamizawa, Development and microstructural characterization of high-thermal-conductivity aluminum nitride ceramics, J. Am. Ceram. Soc. 71 (1988) 588–594.
[10] A.V. Virkar, B.T. Jackson, R.A. Cutler, Thermodynamic and kinetic effect of oxygen removal on the thermal conductivity of aluminum nitride, J. Am. Ceram. Soc. 72 (1989) 2031–2042.
[11] K. Watari, M. Kawamoto, K. Ishizaki, Sintering chemical reactions to increase thermal conductivity of AlN, J. Mater. Sci. 26 (1991) 4727–4732.
[12] M. Hirano, K. Kato, T. Isobe, T. Hirano, Sintering and characterization of fully dense AlN ceramics, J. Mater. Sci. 28 (1993) 4725–4730.
[13] Y.D. Yu, A.M. Hundere, R. Høier, R.E. Dunin-Borkowski, M.A. Einarsrud, Microstructural characterization and microstructural effects on the thermal conductivity of AlN (Y_2O_3) ceramics, J. Eur. Ceram. Soc. 22 (2002) 247–252.
[14] L. Qiao, H. Zhou, K. Chen, R. Fu, Effects of Li_2O on the low temperature sintering and thermal conductivity of AlN ceramics, J. Eur. Ceram. Soc. 23 (2003) 1517–1524.
[15] X. Xu, H. Zhuang, W. Li, S. Xu, B. Zhang, X. Fu, Improving thermal conductivity of Sm_2O_3-doped AlN ceramics by changing sintering conditions, Mater. Sci. Eng. A342 (2003) 104–108.
[16] K.A. Khor, L.G. Yu, Y. Murakoshi, Spark plasma sintering of Sm_2O_3-doped aluminum nitride, J. Eur. Ceram. Soc. 25 (2005) 1057–1065.
[17] C.U. Hsieh, C.N. Lin, S.L. Chung, J. Cheng, D.K. Agrawal, Microwave sintering of AlN powder synthesized by a SHS method, J. Eur. Ceram. Soc. 27 (2007) 343–350.
[18] Kanthal Super Handbook, Kanthal AB, Sweden, 1999.
[19] D.R. Stull, H. Prophet, JANAF thermochemical table—second edition, Natl. Stand. Ref. Data Ser., U.S. Natl. Bur. Stand. (1971).
[20] M.W. Chase Jr., C.A. Davis, J.R. Downney Jr., D.J. Frurip, R.A. Mcdonald, A.N. Syverud, JANAF thermodynamical tables—third edition, J. Phys. Chem. Ref. Data 14 (Suppl. nos. 1 and 2) (1985).
[21] K. Watari, M.E. Brito, M. Yasuoka, M.C. Valecillos, S. Kanzaki, Influence of powder characteristics on sintering process and thermal conductivity of aluminum nitride ceramics, J. Ceram. Soc. Jpn. 103 (1995) 890–891.
[22] J.Y. Qiu, Y. Hotta, K. Watari, K. Mitsuishi, M. Yamazaki, Low-temperature sintering behavior of the nano-sized AlN powder achieved by superfine grinding mill with Y_2O_3 and CaO additives, J. Eur. Ceram. Soc. 26 (2006) 385–390.
[23] J.Y. Qiu, Y. Hotta, K. Watari, Enhancement of densification and thermal conductivity in AlN ceramics by addition of nano-sized particles, J. Am. Ceram. Soc. 89 (2006) 377–380.
[24] P.S. Baranda, A.K. Knudsen, E. Ruh, Effect of CaO on the thermal conductivity of aluminum nitride, J. Am. Ceram. Soc. 76 (1993) 1751–1760.